Dynamics of a Satellite with Flexible Appendages in the Coulomb Interaction

Vladimir S. Aslanov[1]
Samara National Research University, Samara, Russia

Nomenclature

m = mass of the defunct satellite (space debris), kg

J = moment of inertia of the space debris, kg m^2

l_a = length of the flexible appendage (panel), m

l_q = distance between the attachment points of the flexible appendages and Coulomb forces application points, m

R = distance between the mass center of the debris and the fixing points of the flexible appendages, m

$l = l_q + R$

$k_c = 8.99 \times 10^9 \; Nm^2 / C^2$ = Coulomb's constant

$E_a J_a$ = stiffness of the flexible appendages, Nm^2

μ = linear mass of the panel, kg m^{-1}

$O_0 x_0 y_0$ = orbital frame

p_1, p_2 = dimensionless transverse displacement of the flexible panels

$\mathbf{V}_C$ = velocity of the space debris in the frame $O_0 x_0 y_0$

θ = pitch attitude angle

θ_s = stable equilibrium position

θ_u = unstable equilibrium position

I. Introduction

Electrostatic actuation in space has been proposed as early as 1966 by Cover et. al. [1]. Electrostatic force actuation for spacecraft formation control is a concept that is gaining significant attention in the field of formation flying [2,3]. Later Coulomb formation flying dynamics and control has been studied in numerous publications, for example [4-7]. Non-cooperative electrostatic control sees application in orbital space debris mitigation for bodies

[1] Head of Theoretical Mechanics Department, 34 Moskovskoe sh., Samara, 443086, Russia;
aslanov_vs@mail.ru; http://www.aslanov.ssau.ru/

such as defunct satellites. Orbital servicing is a challenging space mission concept that requires an active host vehicle to approach and mechanically interface with the defunct satellite or satellite component [8-11]. Multi-Sphere Method (MSM) is significant for its study of the behavior of bodies under the influence of the Coulomb forces. This method represents the complete spacecraft electrostatic charging model as a collection of spherical conductors dispersed through the body [8] to provide consistentcy between induced charging effects and finite element methods. Multi-Sphere Method can be applied for the cylindrical body and for the body with attached flexible elements as shown in Fig. 1a. Visible are the electrostatic forces between spheres, the projection angle for the torque controller, and the inertial station keeping thrust. The three-sphere MSM approximation provides sufficient force and torque accuracy, within a percent of the finite element solution, for the considered separation distances [11]. The first step in the formulation of this problem was made Schaub and Stevenson, who showed a satellite with solar panels under the influence of Coulomb forces in Fig. 1 at the paper [8].

The aim of the paper is study of influence of flexible appendages on the satellite motion in the Columb interaction. The paper provides the mathematical formulations of Lagrangian dynamics to demonstrate insightful analysis of the full rotating, translating, and flexing system. The work presents chaotic behavior that arises and additional reductions in the complete formulation to consider rigid body motion. The paper examines the possibility of the chaos in the attitude motion caused by small oscillations of the flexible appendages. The paper includes numerical simulations of the full dynamical system and the chaotic behavior cases. The equations of the planar motion of the satellite with the flexible appendages under the influence of Coulomb forces are obtained. Next, the satellite with the flexible appendages is considered as a rigid body. It is showed that in this case there are a stable and an unstable equilibrium positions. And deterministic chaos arises in a vicinity of the unstable equilibrium position in the presence of small perturbations in the form of oscillations of the flexible appendages. This research is important for understanding the influence of Coulomb forces on the motion of the mass center of the space debris with the flexible appendages.

II. Mathematical Models

A. The Three-sphere Electrostatic Model

According to [8] the three-sphere Multi- Sphere Method is a means to approximate the electrostatic interactions between conducting objects with generic geometries. For the Coulomb force's descriptions, the parameter designations are chosen as in [9]. Fig. 1 depicts a satellite with flexible appendages, modeled by 3 optimally placed spheres, in the vicinity of the active satellite as a thrust source. Both objects are assumed for now to be conducting and reside at voltage levels Φ_1 and Φ_2. The voltage Φ_i on a given sphere is a function of the charge q_i on that sphere and the charges on its neighboring spheres. This relation is governed by Eq. (4) [8], where R_i represents the radius of the sphere in question and $r_{i,j} = r_j - r_i$ is the center-to-center distance to each neighbor. The constant $k_c = 8.99\times10^9\ Nm^2 / C^2$ is Coulomb's constant.

$$\Phi_i = k_c \frac{q_i}{R_i} + \sum_{j=1,\, j\neq i}^{m} k_c \frac{q_j}{r_{i,j}} \tag{1}$$

These relations can be combined for each sphere to obtain the matrix equation

$$\begin{bmatrix} \Phi_1 \\ \Phi_2 \\ \Phi_2 \\ \Phi_2 \end{bmatrix} = k_c \left[C_M\right]^{-1} \begin{bmatrix} q_1 \\ q_a \\ q_b \\ q_c \end{bmatrix} \tag{2}$$

where

$$\left[C_M\right]^{-1} = \begin{bmatrix} 1/R_1 & 1/r_a & 1/r_b & 1/r_c \\ 1/r_a & 1/R_{2,a} & 1/l & 1/2l \\ 1/r_b & 1/l & 1/R_{2,b} & 1/l \\ 1/r_c & 1/2l & 1/l & 1/R_{2,c} \end{bmatrix} \tag{3}$$

By inverting $\left[C_M\right]^{-1}$, the charge on each sphere is determined at any instance of time. The charge redistribution and interaction with the space environment are assumed to be orders of magnitude faster than the spacecraft motion. The total electrostatic force is then given by the summations [8]

$$\mathbf{F}_2 = -\mathbf{F}_1 = k_c \left|q_1\right| \sum_{i=a}^{c} \frac{q_i}{r_i^3} \mathbf{r_i} \tag{4}$$

and for each of the three spheres of the object 2

$$\mathbf{F}_{2,i} = k_c \frac{\left|q_1\right| q_i}{r_i^3} \mathbf{r_i}, \qquad i = a,b,c \tag{5}$$

(a)

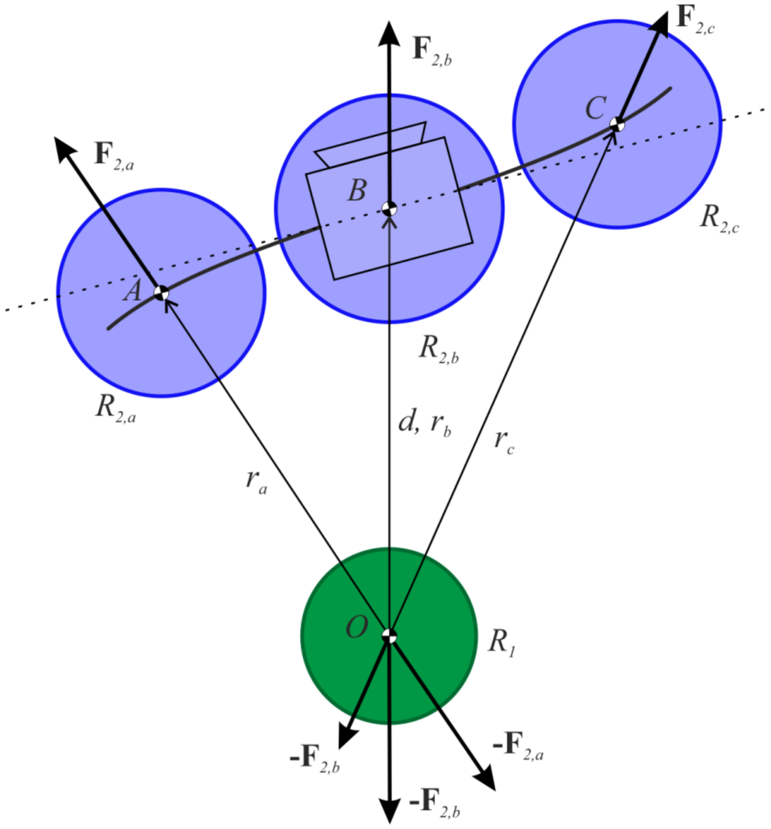

(b)

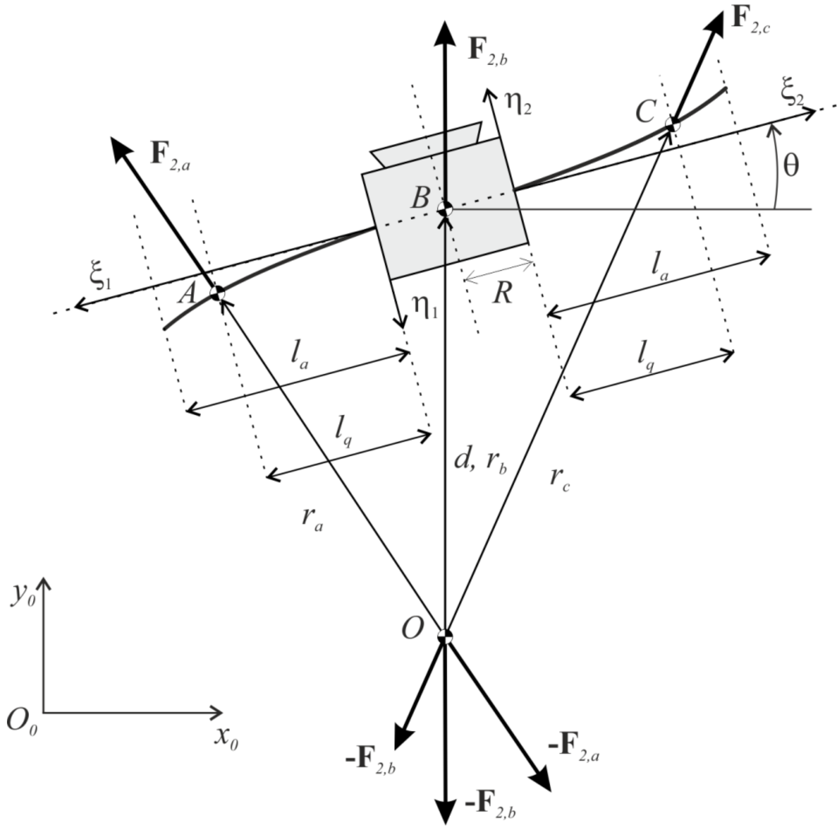

Fig. 1 The three-sphere model (a), frames, forces, coordinates (b)

The studied mechanical system includes the active satellite (space pusher), considered as a particle and the defunct satellite (space debris), as a rigid body with two flexible appendages. We suppose that the attitude motion of the space pusher is controlled by its attitude control system. We consider planar motion of the space debris around its center of mass and this center mass under the influence of only the Coulomb forses. We also assume that the distance between the bodies is fixed $\left(r_b = d = const\right)$, which is provided by an active satellite propulsion. Fig. 1a and equation (5) show that the stable position of the satellite corresponds to the pitch attitude angle $\theta = 0$. Fig. 1b illustrates the geometry of the mechanical system relative to an orbital frame $O_0x_0y_0$ which is assumed to be fixed for a short period in comparison with the orbital period of the system.

B. The Kinetic Energy and the Potential Energy

The kinetic energy of the space debris is composed of the kinetic energy of the rigid body T_b and the kinetic energy of the flexible appendages T_a

$$T = T_b + T_a \tag{6}$$

The kinetic energy of the space debris is written as

$$T_b = \frac{1}{2}\left(m\mathbf{V}_B^2 + J\dot{\theta}^2\right) \tag{7}$$

where m is mass of the space debris, J is a moment of inertia of the space debris, θ is a pitch attitude angle.

The velocity of the space debris in the frame $O_0x_0y_0$ is

$$\mathbf{V}_B = \begin{bmatrix} \dot{x} \\ \dot{y} \end{bmatrix} \tag{8}$$

The kinetic energy of the flexible appendages is

$$T_a = \frac{1}{2}\int_0^{l_a}\left(V_{a1}^2 + V_{a2}^2\right)dm \tag{9}$$

where l_a is the length of the flexible appendage (panel), $\mathbf{V}_{ai}$ is the velocity of a differential mass element dm of the flexible appendage $i = 1, 2$. According to Fig. 1b, velocity of the element dm is

$$\mathbf{V}_{a1} = \mathbf{V}_B + \frac{d}{dt}\left[\begin{pmatrix} \cos\theta & -\sin\theta \\ \sin\theta & \cos\theta \end{pmatrix}\left([-R, 0]^T + [-\xi_1, -\eta_1]^T\right)\right] \tag{10}$$

$$\mathbf{V}_{a2} = \mathbf{V}_B + \frac{d}{dt}\left[\begin{pmatrix} \cos\theta & -\sin\theta \\ \sin\theta & \cos\theta \end{pmatrix}\left([R, 0]^T + [\xi_2, \eta_2]^T\right)\right] \tag{11}$$

where R is the distance between the mass center of the debris and the fixing points of the flexible appendages, ξ_i, η_i are the longitudinal and transverse coordinates for the differential mass element dm of the flexible appendage $i = 1, 2$ (Fig.1b). The deflection of the flexible appendage is defined as

$$\eta_i = \sum_{j=1}^{N}\Phi_j(\xi_i)\,p_{ij}(t), \quad i = 1, 2 \tag{12}$$

where $p_{ij}(t)$ are modal coordinates, N is the number of the assumed modes considered, and $\Phi_j(\xi_i)$ are shape functions. The following shape function is an acceptable candidate for a clamped beam [12, Table 9.4]

$$\Phi_j(\xi_i) = C_j \left[\cosh \frac{\omega_j^{1/2} \xi_i}{l_i} - \cos \frac{\omega_j^{1/2} \xi_i}{l_i} - d_j \left(\sinh \frac{\omega_j^{1/2} \xi_i}{l_i} - \sinh \frac{\omega_j^{1/2} \xi_i}{l_i} \right) \right] \tag{13}$$

where C_j is an unessential constant multiplier which is taken so that $\Phi_j(l_a) = 1$,

$$d_j = \frac{\cos \omega_j^{1/2} + \cosh \omega_j^{1/2}}{\sin \omega_j^{1/2} + \sinh \omega_j^{1/2}}$$

where ω_j is a nondimensional natural frequency. For the fixed-free beam ω_j defined by the equation [19]

$$\cos \omega_j^{1/2} \cosh \omega_j^{1/2} = -1 \tag{14}$$

where $\omega_1 = 3.51, \omega_2 = 22.03, \omega_3 = 61.70, \ldots$ are roots of the equation (14).

The potential energy of the space debris equals the potential energy of the flexible appendages that are considered as beams, and it can be written as

$$U = U_a = \int_0^{l_a} \left[\sum_{i=1}^{2} E_a J_a \left(\frac{\partial^2 \eta_i}{\partial \xi_i^2} \right)^2 \right] d\xi_i \tag{15}$$

where $E_a J_a$ is stiffness of the flexible appendages, η_i is defined from the equation (12).

C. Lagrange Motion Equations of the Center Mass and of Attitude Motion

We use the Lagrangian formalism to write the motion equations of the system

$$\frac{d}{dt}\frac{\partial L}{\partial \dot{s}_j} - \frac{\partial L}{\partial s_j} = Q_j, \quad j = 1, \ldots, 3 + 2N \tag{16}$$

where $L = T - U$ is the Lagrange function, $s_j = x, y, \theta, p_{11}, p_{21}, \ldots p_{1N}, p_{2N}$ are the generalized coordinates, Q_i are generalized force corresponding to the generalized coordinate s_j.

We consider only the case when $N = 1$, and taking into account (6) - (15) the Lagrange function can be written as

$$L = \left(\mu l_a + \frac{m}{2} \right) \left(\dot{x}^2 + \dot{y}^2 \right) + \left[\frac{J}{2} + \mu l_a \left(R l_a + \frac{l_a^2}{3} + R^2 \right) \right] \dot{\theta}^2 + \mu l_a \left(\mathrm{I}_3 + \mathrm{I}_1 R \right) \left(\dot{p}_1 + \dot{p}_2 \right) \dot{\theta}$$

$$+ \mu l_a \mathrm{I}_1 \left(\dot{p}_1 - \dot{p}_2 \right) \left(\dot{x} \sin \theta - \dot{y} \cos \theta \right) + \frac{1}{2} \mathrm{I}_2 \mu l_a^2 \left(\dot{p}_1^2 + \dot{p}_2^2 \right) - \frac{1}{2} E_a J_a \mathrm{I}_4 \left(p_1^2 + p_2^2 \right) \tag{17}$$

where μ is a linear mass of the panel, $p_1 = p_{11} / l_a, p_2 = p_{21} / l_a$ are the dimensionless transverse displacement of the flexible panels [13]

$$I_1 = \int_0^{l_a} \Phi_1(\xi) d\xi \tag{18}$$

$$I_2 = \int_0^{l_a} \Phi_1^2(\xi) d\xi \tag{19}$$

$$I_3 = \int_0^{l_a} \xi \Phi_1(\xi) d\xi \tag{20}$$

$$I_4 = \int_0^{l_a} \left[\Phi_1''(\xi) \right]^2 d\xi \tag{21}$$

$$\Phi_1(\xi) = \cosh \frac{\omega^{1/2}\xi}{l_a} - \cos \frac{\omega^{1/2}\xi}{l_a} - d_1 \left(\sinh \frac{\omega^{1/2}\xi}{l_a} - \sinh \frac{\omega^{1/2}\xi}{l_a} \right) \tag{22}$$

where $\omega = 3.51, d_1 = 0.81$. Note, that exact closed form results are available in the literature, for integrals (18) to (21) for clamped-free beam modes such as the one given in (22) as well as for other boundary conditions [13]. Since these integrals are calculated only once for a panel, therefore it does not have a great value how to calculate them analytically or numerically.

Next, taking into account (5) we define the generalized forces as

$$Q_j = \sum_{i=a}^{c} \frac{\partial \mathbf{r}_i}{\partial s_j} \cdot \mathbf{F}_{2i}, \qquad j = 1, 2, ...5 \tag{23}$$

These equations are non-trivial due to the complexity of the determining Coulomb forces (5) by the matrix (2) and (3), and to obtain analytical solutions we used the symbolic manipulator MATHEMATICA [14]. After some additional transformations the generalized forces (23) are written as

$$\begin{aligned}
Q_\theta\left(\theta, p_1, p_2\right) = {} & \frac{2\Phi^2 dlR_1}{HG_- G_+}(-2d^2 lG_-^2 G_+(al\cos\theta - p_2(l + a\sin\theta)\Phi_q l_a)R_1 R_{2,a}(l - R_{2,b})R_{2,c} + \\
& d(G_-^3 R_1 R_{2,a}(2dl(al\cos\theta - p_2(l + a\sin\theta)F_q l_a)(l - R_{2,b}) - G_+(dl\cos\theta - \\
& p_2(l + d\sin\theta)F_q l_a)(dl - (2d + l)R_{2,b}))R_{2,c} - G_-^4(-G_+(al\cos\theta - p_2(l + a\sin\theta)\Phi_q l_a) \\
& (-2l + R_{2,a})(-d^2 l + (d^2 + dR_1 + lR_1)R_{2,b}) - 2d(dl\cos\theta - p_2(l + d\sin\theta)\Phi_q l_a)R_1 \\
& (dl^2 + (l^2 - (d + l)R_{2,a})R_{2,b}))R_{2,c} - G_- G_+^2 R_{2,a}(-G_+^2(al\cos\theta + p_1(l - a\sin\theta)\Phi_q l_a) \\
& (-d^2 l + (d^2 + dR_1 + lR_1)R_{2,b})(2l - R_{2,c}) - 2d^2 l(al\cos\theta + p_1(l - a\sin\theta)\Phi_q l_a)R_1(l - R_{2,b})R_{2,c} - \\
& dG_+(dl\cos\theta + p_1(l - d\sin\theta)F_q l_a)R_1(dl - (2d + l)R_{2,b})R_{2,c}) - 2d(G_+^2)^{3/2} R_1 R_{2,a}(dl(al\cos\theta + \\
& p_1(l - a\sin\theta)F_q l_a)(l - R_{2,b})R_{2,c} + G_+(dl\cos\theta + p_1(l - d\sin\theta)\Phi_q l_a)(dl^2 + R_{2,b}(l^2 - (d + l)R_{2,c})))) \\
& (2dlG_+ R_{2,a}(l - R_{2,b})(2l - R_{2,c}) + G_-(2dl(2l - R_{2,a})(l - R_{2,b})R_{2,c} + G_+(dl(4l^2 - R_{2,a}R_{2,c}) + \\
& R_{2,b}(4l(l^2 - (d + l)R_{2,c}) + R_{2,a}(-4l(d + l) + (4d + 3l)R_{2,c}))))),
\end{aligned} \tag{24}$$

$$\begin{aligned}
Q_{p_1}\left(\theta\right) = {} & -\frac{2\Phi^2 \Phi_q d^2 l_a l L_1 R_1 R_{2,a} G_+}{HG_-}\cos\theta(dR_1(2dlG_+(l - R_{2,b}) + G_-(2dl(-l + R_{2,b}) + \\
& G_+(-dl + (2d + l)R_{2,b})))R_{2,c} + G_+^2(G_-(d^2 l - (d^2 + dR_1 + lR_1)R_{2,b})(2l - R_{2,c}) + 2dR_1(dl^2 + \\
& R_{2,b}(l^2 - (d + l)R_{2,c})))(2dlG_+ R_{2,a}(l - R_{2,b})(2l - R_{2,c}) + G_-(2dl(2l - R_{2,a})(l - R_{2,b})R_{2,c} +
\end{aligned}$$

$$G_+(dl(4l^2 - R_{2,a}R_{2,c}) + R_{2,b}(4l(l^2 - (d+l)R_{2,c}) + R_{2,a}(-4l(d+l) + (4d+3l)R_{2,c}))))) , \tag{25}$$

$$Q_{p_2}(\theta) = \frac{2\Phi^2\Phi_q d^2 l_a l L_1 R_1 R_{2,a} G_-}{HG_+}\cos\theta (G_-^2(G_+(2l - R_{2,a})(d^2 l - (d^2 + dR_1 + lR_1)R_{2,b}) +$$
$$2dR_1(dl^2 + (l^2 - (d+l)R_{2,a})R_{2,b})) + dR_1 R_{2,a}(2dlG_+(-l + R_{2,b}) + G_-(2dl(l - R_{2,b}) +$$
$$G_+(-dl + (2d+l)R_{2,b}))))R_{2,c}(2dlG_+ R_{2,a}(l - R_{2,b})(2l - R_{2,c}) + G_-(2dl(2l - R_{2,a})(l - R_{2,b})R_{2,c} +$$
$$G_+(dl(4l^2 - R_{2,a}R_{2,c}) + R_{2,b}(4l(l^2 - (d+l)R_{2,c}) + R_{2,a}(-4l(d+l) + (4d+3l)R_{2,c}))))) \tag{26}$$

where

$$G_\pm = \left(l^2 \pm 2ld\sin\theta + d^2\right)^{1/2} ,$$

$$H = k_c\Big[4dlR1G_+R_{2,a}\left(-dG_-\left(l - 2R_{2,b}\right)R_{2,c} + G_+\left(G_-R_{2,b}\left(-2l + R_{2,c}\right) + d\left(l^2 - R_{2,b}R_{2,c}\right)\right)\right) +$$
$$G_-^2\left(4dlR1\left(G_+\left(-2l + R_{2,a}\right)R_{2,b} + d\left(l^2 - R_{2,a}R_{2,b}\right)\right)R_{2,c} + G_+^2\left(d^2 l\left(-4l^2 + R_{2,a}R_{2,c}\right) +\right.\right.$$
$$\left.\left.R_{2,b}\left(4l\left(l^2 R1 + d^2 R_{2,c}\right) + R_{2,a}\left(4d^2 l - \left(4d^2 + lR1\right)R_{2,c}\right)\right)\right)\right)\Big]^2 ,$$

$$\Phi_q = \Phi_1(\xi = l_q) \approx \frac{\omega l_q^{\,2}}{l_a^{\,2}} - \frac{d_1\omega^{3/2} l_q^{\,3}}{3l_a^{\,3}} \quad \left(\omega = 3.51,\, d_1 = 0.81\right) \tag{27}$$

The torque of the Coulomb forces (24) is the cause of the oscillatory motion of the satellite. Equation (27) determines the approximate value of the function (22) [15, Eq. (34)] for the centers of the spheres A and C.

For this manuscript's simulations, system parameters are chosen as in Table 1. Assume first that both bodies have the same potential magnitude $\Phi_2 = |\Phi_1|$. Figs. 2, 3 shows the time history of the pitch attitude angle θ and $k_c|q_1|q_a$ (dotted line), $k_c|q_1|q_c$ (solid line) at various separation distances $d = 15m$ and $d = 3.2m$. The initial conditions are chosen as:

$$\theta_0 = \frac{\pi}{2} - 0.5,\ \dot{\theta}_0 = 0,\ p_1 = 0.1,\ \dot{p}_1 = 0.000227,\ p_2 = 0,\ \dot{p}_2 = 0 \tag{28}$$

Table 1 Parameters of the system

Parameter	Value	Parameter	Value	Parameter	Value
$J,\ kgm^2$	1000	$l,\ m$	1.1569	$\mu,\ kgm^{-1}$	10
$\Phi_2 = \lvert\Phi_1\rvert, kW$	20	$l_a,\ m$	2	E_aJ_a, Nm^2	9.2
$R_1,\ m$	0.5	$R_{2,a} = R_{2,c},$	0.5909	$R_{2,b}, m$	0.5909
$R,\ m$	0.5				

(a)

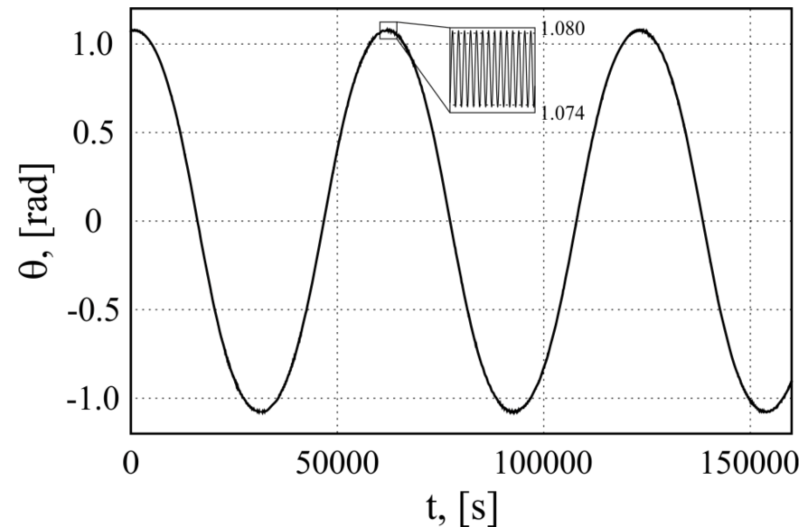

(b)

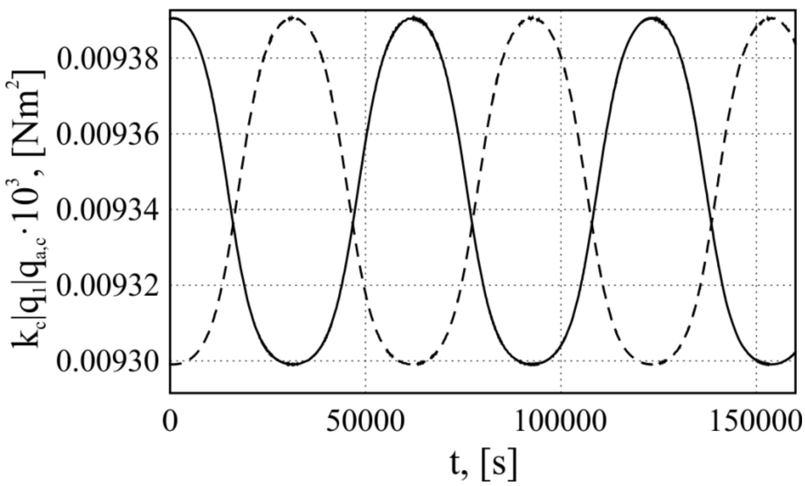

Fig. 2 Time history of the pitch attitude angle θ (a) and $k_c|q_1|q_a$ (dotted line), $k_c|q_1|q_c$ (solid line) (b) for $d = 15m$

(a)

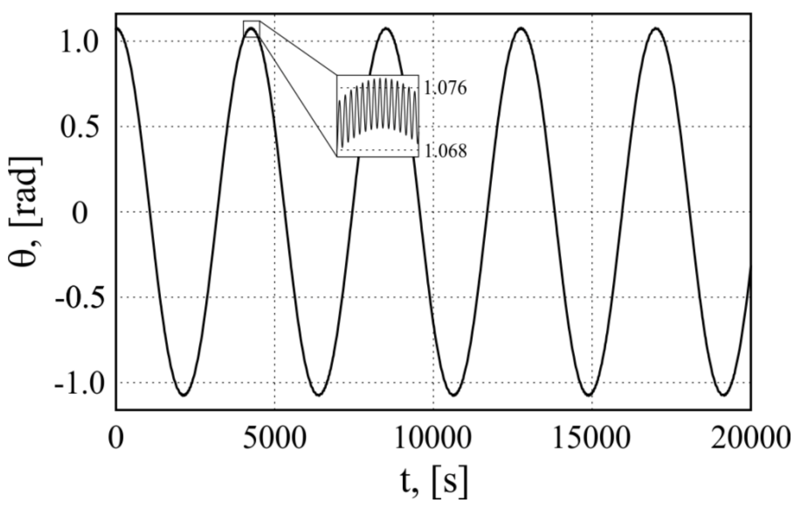

(b)

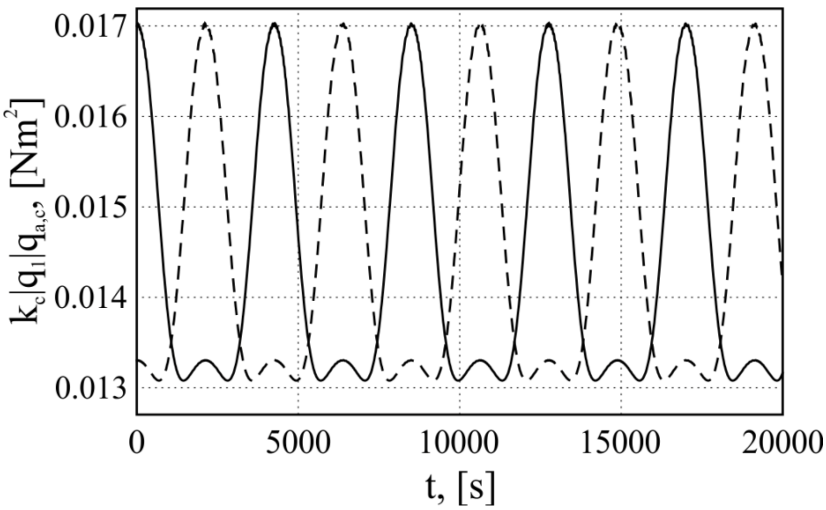

Fig. 3 Time history of the pitch attitude angle θ (a) and $k_c|q_1|q_a$ (dotted line), $k_c|q_1|q_c$ (solid line) (b) for $d = 3.2\,m$

It can be seen a in-zoom (Figs.2a and 3a) that the pitch angle oscillations have a high-frequency harmonic of small amplitude caused by the flexible appendages. Under certain conditions, when the pitch attitude angle θ is in a small neighborhood of unstable equilibrium positions $\theta_u = \pm\frac{\pi}{2}$, the behavior can become chaotic. This will be shown in section IV below.

The pitch torque is created two electrostatic forces

$$\mathbf{F}_{2,a} = k_c|q_1|q_a\frac{\mathbf{r_a}}{r_a^3}, \qquad \mathbf{F}_{2,c} = k_c|q_1|q_c\frac{\mathbf{r_c}}{r_c^3} \tag{29}$$

And the parameters

$$k_c|q_1|q_a\ , \quad k_c|q_1|q_c \tag{30}$$

are determined the flow of an electrostatic charge due of the pitch attitude angle θ. Figs. 2, 3 shows that for the longer distance $d = 15\,m$ these parameters vary slightly with time, and hence with the pitch attitude angle. In the future, this property will allow us to simplify the equations of the attitude motion.

III. The satellite as rigid body. Phase Equilibrium Positions and Space Trajectories

A motion will be called the Rigid Body Motion if the satellite has the absolutely rigid appendages

$$p_1 \equiv 0,\ \ p_2 \equiv 0 \tag{31}$$

In this case the Lagrangian (17) is written as

$$L = \frac{J_*}{2}\dot{\theta}^2 \tag{32}$$

where a_θ is the generalized mass

$$a_\theta = J + 2\mu l_a\left(Rl_a + \frac{l_a^2}{3} + R^2\right) \tag{33}$$

and one can write down generalized force as

$$Q_\theta = \sum_{i=a}^{c}\frac{\partial \mathbf{r}_i}{\partial s_j}\cdot\mathbf{F}_{2i} = -\left|\overrightarrow{BA}\times\mathbf{F}_{2,a}(\theta)\right| + \left|\overrightarrow{BC}\times\mathbf{F}_{2,c}(\theta)\right| \tag{34}$$

which as can be seen from Fig. 1 becomes zero at the points

$$\theta_* = \pm k\frac{\pi}{2}, \qquad (k = 0,1,2,...)$$

Fig. 4 depicts the phase trajectories for the Rigid Body Motion. Obviously the points

$$\theta_s = 0 \pm k\pi \tag{35}$$

correspond to the stable equilibrium position, and the points,

$$\theta_u = \frac{\pi}{2} \pm k\pi \tag{36}$$

correspond to the unstable equilibrium position.

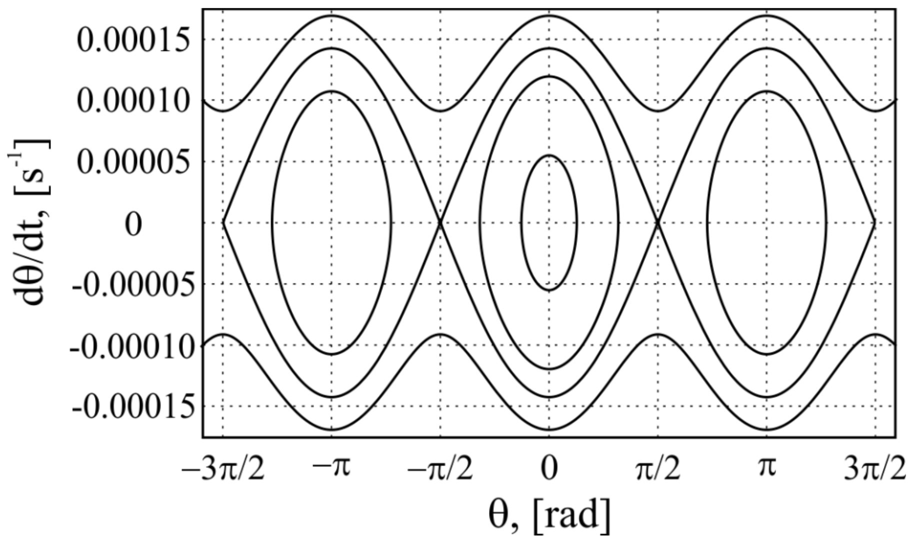

Fig. 4 The phase trajectories $\dot{\theta}(\theta)$ **for** $d = 15m$

The action of small perturbations, as shown in Fig. 2a, caused by transverse vibrations of the flexible appendages in the vicinity of unstable equilibrium positions can lead to deterministic chaos.

IV. Chaotic behavior of the Satellite with Flexible Appendages

As in Section II, we consider the motion of the satellite with flexible appendages. One can illustrate the deterministic chaos by considering a trajectory that starts in a small neighborhood of an unstable equilibrium position (36)

$$\theta_0 = \frac{\pi}{2} - 0.005,\ \dot{\theta}_0 = 0,\ p_1 = 0.1,\ \dot{p}_1 = 0.000227,\ p_2 = 0,\ \dot{p}_2 = 0 \tag{37}$$

The system parameters are chosen as in Table 1. We also set the separation distance $d = 3.2m$. Fig. 5 shows that during a period of 50,000 sec, the satellite with flexible appendages performed rotation in different directions and oscillations in different phase areas:

$$1.\ \theta \in \left(-\frac{\pi}{2}, \frac{\pi}{2}\right) \Rightarrow 2.\ \theta \in \left(\frac{13\pi}{2}, \frac{15\pi}{2}\right) \Rightarrow 3.\ \theta \in \left(\frac{11\pi}{2}, \frac{13\pi}{2}\right) \Rightarrow 4.\ \theta \in \left(\frac{13\pi}{2}, \frac{15\pi}{2}\right) \Rightarrow$$

$$5.\ \theta \in \left(\frac{7\pi}{2}, \frac{9\pi}{2}\right) \Rightarrow 6.\ \theta \in \left(\frac{9\pi}{2}, \frac{11\pi}{2}\right) \Rightarrow 7.\ \theta \in \left(\frac{5\pi}{2}, \frac{7\pi}{2}\right) \Rightarrow 8.\ \theta \in \left(\frac{11\pi}{2}, \frac{13\pi}{2}\right)$$

Note, if there were no flexible oscillations of the attached appendages, then the satellite would oscillate relative to a stable equilibrium position $\theta_s = 0$ in the area 1 and remain there always. Consequently, a tumbling of the satellite, which we see in Fig. 5, is caused by the small oscillations of the appendages.

(a)

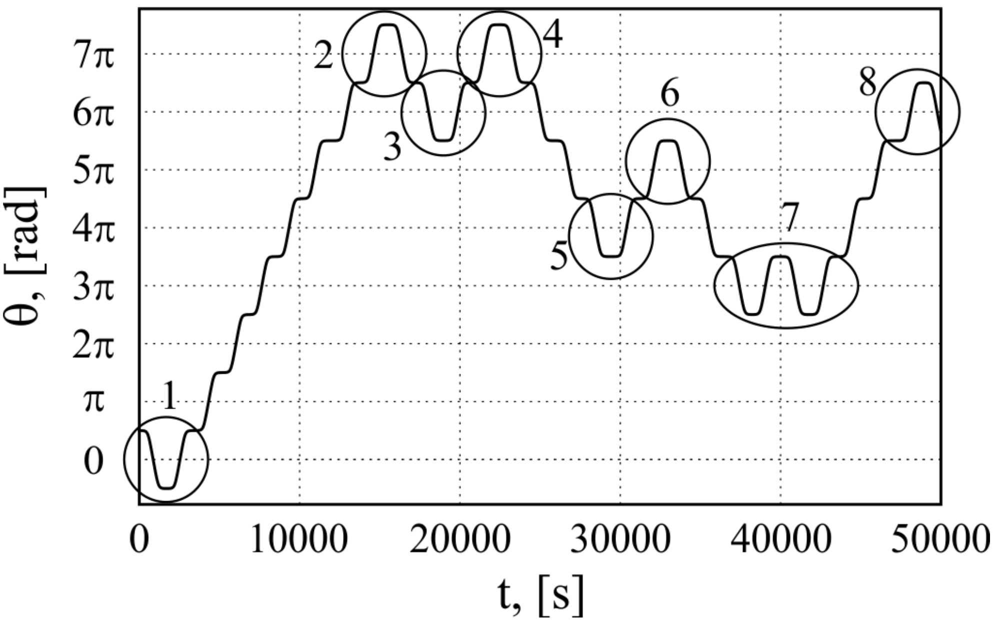

(b)

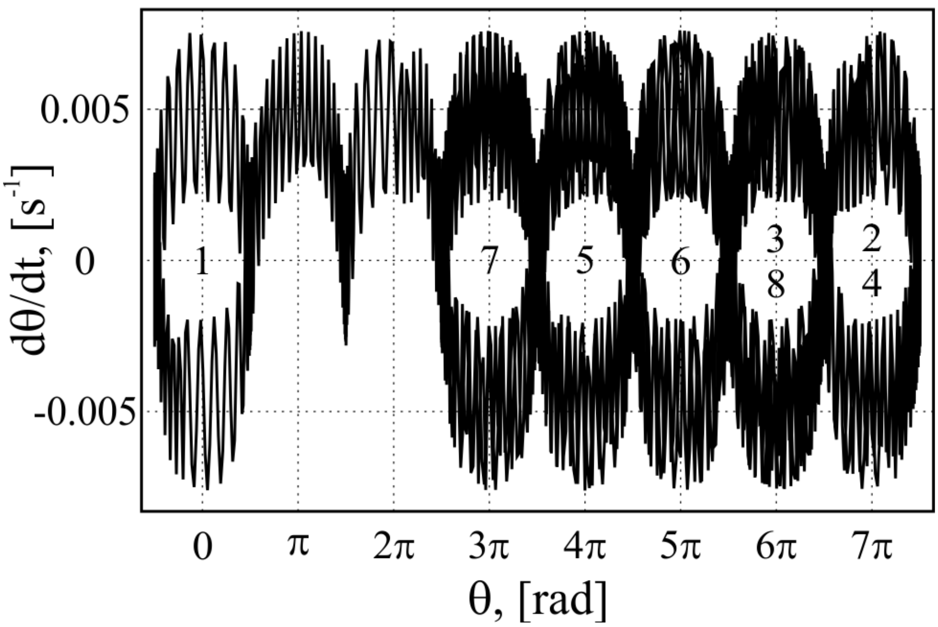

Fig. 5 Time history of the pitch attitude angle θ (a), the phase trajectories $\dot{\theta}(\theta)$ (b)

It can be noted that carrying out a more complete analysis of the chaotic behavior of the system by constructing Poincaré surfaces, computing Lyapunov exponents, or Melnikov functions requires multiple computations of the trajectories.

The three-sphere MSM [8] describes the complex nature of the electrostatic interaction of two bodies. However, the numerical implementation of this method includes complex vector-matrix transformations (2)-(5). This feature of the method leads to large computing times. Therefore, here we confined ourselves to studying only one trajectory of the motion of the satellite with flexible appendages.

V. A Simplified Mathematical Model of the Attitude Motion

Fig. 2b shows that for the distance between the body 1 and 2 $d = 15m$ we can neglect the electrostatic charge flows for a preliminary analysis of the attitude motion of the body 1. We introduce the relative length of the flexible appendages as

$$\lambda = \frac{l}{d} \tag{38}$$

and for

$$\lambda << 1 \tag{39}$$

one can accept that

$$k_c |q_1| q_a = k_c |q_1| q_c = n = const \tag{40}$$

Then the Coulomb forces for the spheres 2a and 2c (Fig. 1) can be given by simple formulas

$$\mathbf{F}_{2,i} = \frac{n}{r_i^3} \mathbf{r_i}, \qquad i = a, c \tag{41}$$

Taking into account (41) for the three generalized coordinates

$$s_j = \theta, p_1, p_2 \tag{42}$$

the generalized forces (23) can be written as

$$Q_\theta = \frac{n\lambda}{d} \cos\theta \left(D_+ - D_- \right)$$

$$+ \frac{n l_a \lambda}{a^2} \Phi_1 \left[p_1 \left(-\lambda + \sin\theta \right) D_- - p_2 \left(\lambda + \sin\theta \right) D_+ \right] \tag{43}$$

$$Q_{p_1} = -\frac{n l_a}{d^2} \Phi_1 D_- \cos\theta \tag{44}$$

$$Q_{p_2} = \frac{n l_a}{d^2} \Phi_1 D_+ \cos\theta \tag{45}$$

where

$$D_\pm = \frac{1}{\left(1 \pm 2\lambda \sin\theta + \lambda^2 \right)^{3/2}} \tag{46}$$

For the three generalized coordinates (42) the Lagrangian (17) takes the form

$$L = \frac{a_\theta}{2} \dot{\theta}^2 + \frac{a_q}{2} \left(\dot{p}_1^2 + \dot{p}_2^2 \right) + a_{\theta q} \left(\dot{p}_1 + \dot{p}_2 \right) \dot{\theta} - \frac{c_q}{2} \left(p_1^2 + p_1^2 \right) \tag{47}$$

where the generalized stiffness of the flexible panels is defined as

$$c_p = E_a J_a \mathrm{I}_4 \tag{48}$$

and the generalized masses can be written as

$$a_p = \mathrm{I}_2 \mu l_a^2 \tag{49}$$

$$a_{\theta p} = \mu l_a \left(\mathrm{I}_3 + \mathrm{I}_1 R\right) \tag{50}$$

The generalized forces (43)-(45) are quite complicated due to the presence in them the square polynomials of negative fractional degree (46). Assuming that (39) is satisfied we expand the generalized forces (43)-(45) in the power series of λ

$$\begin{aligned} Q_\theta = &-c\left[\left(3+\frac{5}{4}\lambda^2\right)\sin 2\theta - \frac{35}{8}\lambda^2 \sin 4\theta\right] \\ &+b\left(p_1 - p_2\right)\left[\sin\theta + \frac{3}{8}\lambda^2\left(3\sin\theta - 5\sin 3\theta\right) + \frac{5}{128}\lambda^4\left(30\sin\theta - 35\sin 3\theta + 63\sin 5\theta\right)\right] \\ &+b\left(p_1 + p_2\right)\left[-\frac{1}{2}\lambda\left(-1+3\cos 2\theta\right) + \frac{1}{16}\lambda^3\left(9 - 20\cos 2\theta + 35\cos 4\theta\right)\right] + O[\lambda]^5 \end{aligned} \tag{51}$$

$$Q_{p_1} = -b\left[\cos\theta + 3\lambda\cos\theta\sin\theta + \frac{3}{8}\lambda^2\left(\cos\theta - 5\cos 3\theta\right)\right] + O[\lambda]^5 \tag{52}$$

$$Q_{p_2} = b\left[\cos\theta - 3\lambda\cos\theta\sin\theta + \frac{3}{8}\lambda^2\left(\cos\theta - 5\cos 3\theta\right)\right] + O[\lambda]^5 \tag{53}$$

where

$$c = n\frac{\lambda^2}{d} \tag{54}$$

$$b = \frac{n l_a}{d^2}\Phi_1 \tag{55}$$

Then the simplified equations of the attitude motion can be written in a very compact form

$$a_{\theta p}\ddot{p}_1 + a_{\theta p}\ddot{p}_2 + a_\theta \ddot{\theta} = Q_\theta \tag{56}$$

$$a_p \ddot{p}_1 + a_{\theta p}\ddot{\theta} = Q_{p_1} - c_p p_1 \tag{57}$$

$$a_p \ddot{p}_2 + a_{\theta p}\ddot{\theta} = Q_{p_2} - c_p p_2 \tag{58}$$

Considering the attached appendages as absolutely rigid $\left(p_1 \equiv 0, p_2 \equiv 0\right)$, we obtain the electrostatic torque as

$$Q_\theta = -c\left[\left(3+\frac{5}{4}\lambda^2\right)\sin 2\theta - \frac{35}{8}\lambda^2\sin 4\theta\right] + O[\lambda]^6 \tag{59}$$

The simulation was performed for the parameters listed in Table 1 and under the initial conditions (28) for separation distances $d = 15m$ $\left(\lambda = l/d = 0.077\right)$. The initial conditions are chosen so that the pitch attitude angle θ remains small:

$$\theta_0 = 0.1,\ \dot{\theta}_0 = 0,\ p_1 = 0.1,\ \dot{p}_1 = 0.000227,\ p_2 = 0,\ \dot{p}_2 = 0$$

Figs. 6 shows the time history of the pitch attitude angle θ and $k_c|q_1|q_a$ (dotted line), $k_c|q_1|q_c$ (solid line) for separation distance $d = 15m$. It follows from Fig. 6b that the functions $k_c|q_1|q_a$ and $k_c|q_1|q_c$ vary periodically about the value $n = 0.009336176\,Nm^2$ and the amplitude of the oscillation is quite small. Fig. 7 shows the results of numerical integration of the simplified Eqs. (56)-(58) and we can see very good agreement with the results of integrating the fully coupled model (16), presented in Fig. 6a.

a)

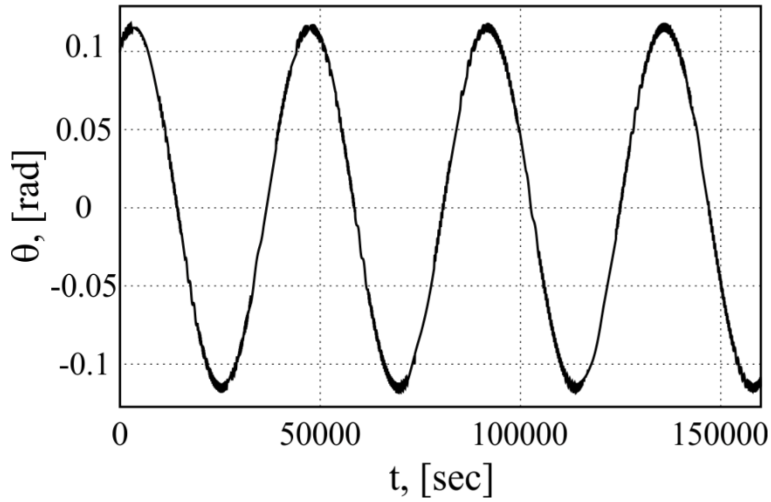

b)

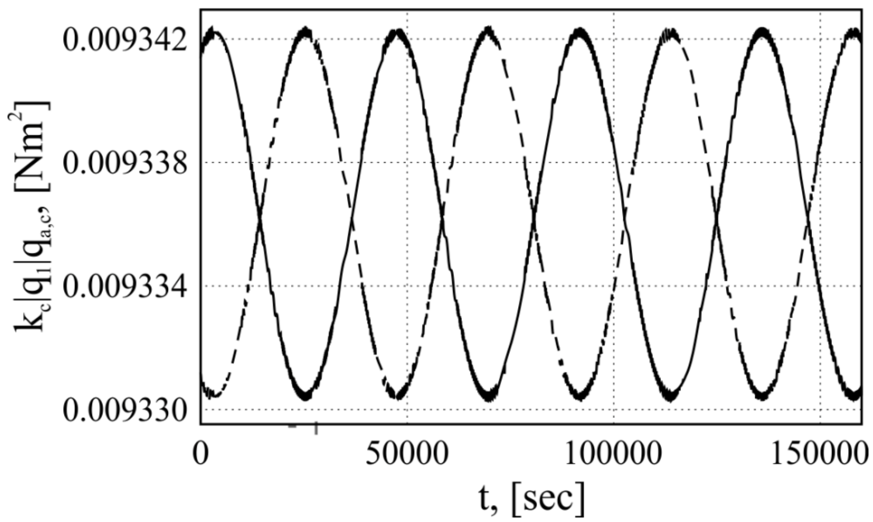

Fig. 6 Time history of the pitch attitude angle θ (a) and $k_c|q_1|q_a$ (dotted line), $k_c|q_1|q_c$ (solid line) (b) for $d = 15m$

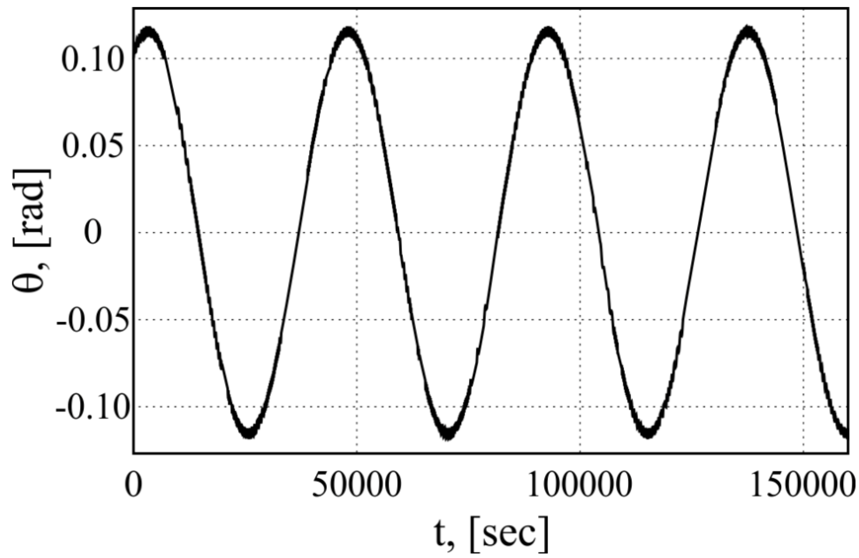

Fig. 7 Time history of the pitch attitude angle θ for the simplified equations (56)-(58)
$$\left(n = 0.009336176\,Nm^2,\ d = 15\,m,\ \lambda = 0.077\right)$$

Note that when using the simplified Eqs. (56)-(58), the computational volume is reduced by an order of magnitude in comparison with the fully coupled model (16).

VI. Conclusion

The attitude dynamics of the defunct satellite with the flexible appendages under action of the Coulomb forces was studied for active space debris removal. An electrostatic interaction is significantly influenced by the relative position of the defunct satellite. Using the multi-sphere method [8], the equations of the planar motion of the satellite with the flexible appendages under the influence of the Coulomb forces were obtained. The main features associated with the influence of the small oscillations of the flexible appendages were identified by numerical simulation of the fully coupled model. Next, the satellite with the flexible appendages is considered as a rigid body. Stable and unstable equilibrium positions were found. By numerical simulation, it was shown that the deterministic chaos arises in the vicinity of an unstable equilibrium position in the presence of small perturbations in the form of oscillations of flexible appendages. This chaos leads to unpredictable consequences, when the satellite with the flexible appendages can begin to tumble. For the case when the separation distance d is much larger than the length of l, the simplified model of the attitude motion was proposed. The use of this model requires considerably less computational costs than the fully coupled model. However this model can be used only in the case of small pitch attitude angle. Otherwise full model presented in Section II should be applied.

In general, we believe that the above research can provide good results for a study an opportunity of the space debris removal by the Coulomb interaction with the active spacecraft. Future work will expand the control to impact general three-dimensional rotational motion.

Acknowledgments

This study was supported by the Russian Foundation for Basic Research (RFBR15-01-01456-A.

References

[1] J. H. Cover, W. Knauer, and H. A. Maurer, “Lightweight Reflecting Structures Utilizing Electrostatic Inflation,” US Patent 3,546,706, October 1966.

[2] King, L. B., Parker, G. G., Deshmukh, S., and Chong, J.-H., “Spacecraft Formation-flying using Inter-vehicle Coulomb Forces,” NASA/NIAC, Technical Rept., http://www.niac.usra.edu, [retrieved Jan. 2002].

[3] King, L.B., Parker, G. G., Deshmukh, S. and Chong J.-H., "Study of Interspacecraft Coulomb Forces and Implications for Formation Flying," *Journal of Propulsion and Power*, 19.3, 2003, pp. 497-505.

[4] Berryman, J., Schaub, H., "Analytical charge analysis for 2- and 3-craft coulomb formations," *Journal of Guidance Control and Dynamics,* 30 (6), 2007, pp. 1701–1710.

[5] Schaub, H., Hall, C., and Berryman, J., “Necessary Conditions for Circularly-Restricted Static Coulomb Formations,” Journal of the Astronautical Sciences, Vol. 54, July-Dec. 2006, pp. 525–541.

[6] Berryman, J.,. Schaub, H., “Static Equilibrium Configurations in GEO Coulomb Spacecraft Formations,” Advances in Astronautical Sciences, Vol. 120, American Astronautical Society, 2005, pp. 51–68. Paper No. AAS 05–104.

[7] Schaub, H., Gordon, G. P., and Lyon B. K., "Challenges and prospects of Coulomb spacecraft formation control," *Journal of Astronautical Sciences,* 52.1, 2004, pp. 169-193.

[8] Stevenson, D., Schaub, H., "Multi-Sphere Method for modeling spacecraft electrostatic forces and torques," *Advances in Space Research,* 51(1), 2013, pp. 10-20.

[9] Schaub, H., Stevenson, D., "Prospects of relative attitude control using coulomb actuation," *The Journal of the Astronautical Sciences*, 60 (3-4), 2013, pp. 258-277.

[10] Bennett, T., Schaub, H., "Touchless Electrostatic Three-dimensional Detumbling of Large Axi-symmetric Debris," *The Journal of the Astronautical Sciences*, 62 (3), 2015, pp. 233-253.

[11] Stevenson, D., Schaub, H., "Optimization of Sphere Population for Electrostatic Multi Sphere Model," In: 12th Spacecraft Charging Technology Conference, Kitakyushu, Japan, May 14–18, 2012.

[12] Kelly, G., *Fundamentals of Mechanical Vibrations*. McGraw-Hill, 2000.

[13] Sharma, C. B. "Calculation of integrals involving characteristic beam functions." Journal of Sound and Vibration, 56(4) 1978, pp. 475-480.

[14] S. Wolfram, S., The Mathematica Book, 5th ed., Cambridge University Press, Cambridge, 2003.

[15] Aslanov, V., Yudintsev V. "Dynamics, analytical solutions and choice of parameters for towed space debris with flexible appendages." Advances in Space Research 55 (2) 2015, pp. 660-667.